 CMC, vol.28, no.2, pp.97-120, 2012

Eigenvalue Analysis of MEMS Components with Multi-defect using Infinite Element Method Algorithm

De-Shin Liu[1,2], Chin-Yi Tu[1] and Cho-Liang Chung[3]

Abstract: Manufacturing defects in the membrane of MEMS (Micro-Electro-Mechanical-Systems) structures have a significant effect on the sensitivity and working range of the device. Thus, in optimizing the design of MEMS devices, it is essential that the effects of membrane defects (e.g., cracks) can be predicted in advance. Accordingly, this study proposes the detailed two-dimensional Infinite Element Method (IEM) formulation with Infinite Element (IE)-Finite Element (FE) coupling scheme for analyzing the out-of-plane vibration of isotropic MEMS membranes containing one or more tip cracks. In the proposed approach, a degenerative computation scheme is used to condense the multiple element layers of the IEM domain to a single layer with master nodes at the boundary only. The validity of the proposed algorithm is demonstrated by comparing the results obtained for the vibration of a rectangular membrane with the analytical solutions and the solutions obtained using the conventional Finite Element (FE) method, respectively. The validated IEM algorithm is then coupled with an FE scheme to analyze various cracked membrane vibration problems. The results show that the fundamental frequency of the membrane changes in accordance with the membrane thickness, but is unaffected by the number of cracks. However, it is shown that a change in the location of the cracks may cause a shift or rotation of the wave peaks of the structural mode shape. In general, the IEM algorithm presented in this paper provides a fast modeling, direct, and accurate tool to simulate the effects of cracks on the dynamic response of MEMS membranes. Furthermore, the algorithm can be easily integrated with experimental methods in order to test for the presence of cracks as part of the MEMS membrane quality control process.

[1] Advanced Institute of Manufacturing for High-tech Innovations and Department of Mechanical Engineering, National Chung Cheng University, 168, University Rd., Min-Hsiung, Chia-Yi, 621, Taiwan, R.O.C.

[2] Corresponding author. Tel.: +886-5-2720411 (Ext: 33305); fax: +886-5-2720589. E-mail address: imedsl@ccu.edu.tw (D.S. Liu).

[3] Department of Materials Science and Engineering, I-Shou University, No. 1, section 1, Shiuecheng Road, Dashu Shiang, Kaohsiung Country, Taiwan, 840, R.O.C.

Keywords: MEMS, membrane vibration, Infinite Element Method, crack problems

1 Introduction

Many MEMS (Micro-Electro-Mechanical-Systems) devices utilize some form of membrane structure to transmit mechanical energy or electronic signals. The performance of such devices is seriously degraded if the membrane contains manufacturing defects such as cracks. Accordingly, reliable methods are required to check the mechanical integrity of the membrane during the quality control process. The dynamic characteristics of MEMS components are commonly evaluated using non-destructive test methods such as the resonant frequency method [Zhang, Uttamchandani, Culshaw and Dobson (1990); Tanner, Walraven and Helgensen (2000)]. The resonant frequency method can also be used to measure the mechanical properties (e.g., Young's modus and internal stress) of silicon micro-resonators in a non-destructive manner. It was shown that a single defect in the membrane affects the structural mode shape, but has no significant effect on the resonant frequency [Gerbach, Ebert and Brokmann (2010)]. In addition to resonance tests, the effects of artificial membrane defects such as sharp cracks are also commonly evaluated by performing Vickers indenter tests [Pugno, Peng and Espinosa (2004)]. In characterizing the response of membrane-based MEMS devices, it is desirable to produce a large number of membranes with identical defect characteristics such that the dynamic response of the device can be reliably determined. However, in practice, making reproducible samples with identical cracks is extremely difficult. As a result, the use of simulation methods to evaluate the frequencies and frequency response of MEMS membranes has become increasingly common in recent years [Ebert, Naumann, Gerbach and Bagdahn (2007); Ricart, Blokhina and Gorreta (2010)]. Simulation methods are relatively straightforward for membranes containing a single crack. However, modeling the dynamic response of membranes with multiple cracks is far more challenging. A method was presented for characterizing the wafer-level membrane structure parameters in the early stages of the MEMS manufacturing process [Michael, Hering, Holzer, Polster, Hoffmann and Albrecht (2006-2007)]. In the proposed approach, the modal response of the membrane structure was measured optically, and the measurement data were then processed by an inverse identification algorithm based on a Finite Element (FE) model in order to identify the membrane parameters (e.g., the membrane thickness). Also, several investigations focus on the improvement of numerical method to predict the effect of the multi-crack problems (e.g., FEM, MFEM and MLPG) [Ramakrishnan, Rao(2005); Nishioka, Tchouikov, Fujimoto (2006); Liu, Long, Li (2008)]. However, it still lack of an efficient modeling process to calculate dynamic response of

membrane with multi-crack.

In this paper, the algorithms derived in previous studies [Ying (1995); Han (1982-1983)] are worked out in detail to construct an IEM numerical procedure, which is extended in combination with FEM for analyzing the out-of-plane vibration of isotropic MEMS membranes with multi-crack. In the proposed approach, a degenerative computation algorithm is used to condense the mass and stiffness matrices of the individual elements around the defect into equivalent global mass and stiffness matrices. Moreover, the individual element layers are consolidated into a single IE super element with master node at the boundary only [Liu and Chiou (2003-2005); Liu, Zhuang, Chung and Chen (2009); Ying (1992)]. The IE super element is applicable to all cracks having the same characteristics (i.e., width and length). Thus, the need to re-mesh the entire problem domain each time an additional crack is introduced to the model is potentially removed. Consequently, the time and complexity of the analysis procedure are significantly reduced. The validity of the proposed approach is confirmed by comparing the results obtained for the vibration of a rectangular membrane with the analytical solutions and the solutions obtained using the conventional FE method, respectively. The applicability of the proposed method is then demonstrated by evaluating the dynamic response of rectangular and circular membranes with and without cracks, respectively. In practice, wave shape may change in accordance with the size, position and number of the membrane defects. In the present study, the change in the wave shape is quantified using a MAC-value parameter (see Eq. (1)), which essentially compares the eigenvectors of the crack-free reference structure (v_r) and the cracked sample structure (v_s), respectively.

$$\mathrm{MAC}(\%) = \frac{\left(v_s^T v_r\right)^2}{\left(v_s^T v_s\right)\left(v_r^T v_r\right)} \times 100\% \tag{1}$$

2 Formulation

2.1 Out-of-plane vibration of rectangular membrane

Consider a rectangular membrane extending over a domain D ($0 < x < a, 0 < y < b$) and having a thickness h (see Fig. 1). Assuming that the mass density ρ of the membrane is constant, the governing equation for the vibration of the membrane has the form shown in Eq. (2), where T is the tension force per unit length of the membrane edge. The Laplacian equation can be expressed in rectangular coordinates as shown in Eq. (3). Meanwhile, the boundary conditions at the fixed edges of the membrane have the forms shown in Eqs. (4) & (5). The differential equation and corresponding boundary conditions collectively constitute the eigenvalue

problems. The solution of this eigenvalue problem consists of the eigenvalues $\beta_{m,n}$ (defined in Eq. (6) and the natural frequency $\omega_{m,n}$ (given in Eq.(7)).

$$-T\nabla^2 W = \rho h \frac{\partial^2 W}{\partial t^2} \tag{2}$$

$$\nabla^2 = \frac{\partial^2}{\partial x^2} + \frac{\partial^2}{\partial y^2} \tag{3}$$

$$W(0,y) = 0, \quad W(a,y) = 0 \tag{4}$$

$$W(x,0) = 0, \quad W(x,b) = 0 \tag{5}$$

$$\beta_{m,n} = \pi \sqrt{\left[\left(\frac{m}{a}\right)^2 + \left(\frac{n}{b}\right)^2\right]} \quad m,n = 1,2,\cdots \tag{6}$$

$$\omega_{m,n} = \pi \sqrt{\left[\left(\frac{m}{a}\right)^2 + \left(\frac{n}{b}\right)^2\right]} \frac{T}{\rho h} \tag{7}$$

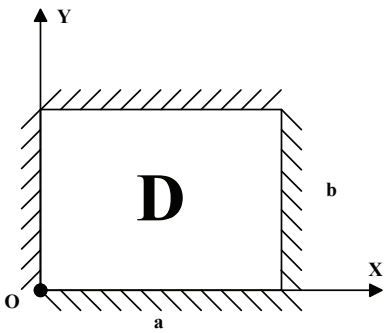

Figure 1: Schematic illustration of rectangular membrane clamped at all four edges

2.2 IEM-FEM coupled scheme

When the problem domain (i.e., membrane) contains multiple cracks, modeling the entire domain using IEM is laborious and computationally complex. Therefore, the present study proposes an IEM-FEM coupled scheme in which the neighborhood region of each crack is sub-divided into similar elements using IEM, while the remainder of the problem domain is meshed using the conventional FE method.

To illustrate the proposed scheme, consider the single crack problem shown in Fig. 2. As shown, the problem domain is partitioned into two sub-domains, Ω and D,

separated by a coupling interface, Γ_0, and modeled by FEM and IEM, respectively. The algebraic assembled element equation for the FE sub-domain is given as follows.

$$[M]\left\{\ddot{X}\right\}+[K]\{X\}=0 \tag{8}$$

where M/K is the mass/stiffness matrix of the FE sub-domain and X is the nodal displacement. Furthermore, Eq. (8) could be written as Eq.(11). Note that the M/K matrix is formulated in Eqs.(9) & (10).

$$[M^e]=\rho h\left\{\int_D \phi_i\phi_j det\,[J]\,d\xi\,d\eta\right\} \tag{9}$$

$$[k^e]=T\left\{\int_D \frac{\partial\phi_i}{\phi\xi}\frac{\partial\phi_j}{\phi\xi}det\,[J]\,d\xi\,d\eta+\int_D \frac{\partial\phi_i}{\phi\eta}\frac{\partial\phi_j}{\phi\eta}det\,[J]\,d\xi\,d\eta\right\} \tag{10}$$

$$\begin{bmatrix} M_{couple} & M_{cf}^T \\ M_{cf} & M_{FEM} \end{bmatrix}\begin{Bmatrix} \ddot{X}_0 \\ \ddot{X}_{FEM} \end{Bmatrix}+\begin{bmatrix} K_{couple} & K_{cf}^T \\ K_{cf} & K_{FEM} \end{bmatrix}\begin{Bmatrix} X_0 \\ X_{FEM} \end{Bmatrix}=0 \tag{11}$$

X_0 and X_{FEM} are the vectors of the IE/FE interface and non-interface nodal displacements, respectively. From Eq. (11), the following equations can be derived:

$$M_{couple}\left\{\ddot{X}_0\right\}+M_{cf}^T\left\{\ddot{X}_{FEM}\right\}+K_{couple}\{X_0\}+K_{cf}^T\{X_{FEM}\}=0 \tag{12}$$

$$M_{cf}\left\{\ddot{X}_0\right\}+M_{fem}\left\{\ddot{X}_{FEM}\right\}+K_{cf}\{X_0\}+K_{FEM}\{X_{FEM}\}=0 \tag{13}$$

2.3 Eigenvalue problem formulation of Infinite Element Method

Utilizing the IEM approach, a very fine mesh pattern can be established around each tip crack without increasing the degree of freedom of the global FEM solution.

For element I, (*xi*,*yi*) denotes the global coordinates of node i, Taking the global origin O and c as the center of the similarity and the proportionality ratio, respectively, a second element (element II) can be created whose nodal coordinate values are similar to those of element I (see Fig. 3).

The relationship between the physical coordinates of the two elements is shown in Eq.(14).

$$\left(x_i^{II},y_i^{II}\right)=c\,(x_i,y_i) \tag{14}$$

Equations (15) - (17) show that shape functions are used to express the coordinates of a point within elements I and II in terms of the nodal coordinates.

$$\begin{cases} x^I=\sum_{i=1}^4 \phi_i x_i^I \\ y^I=\sum_{i=1}^4 \phi_i y_i^I \end{cases} \tag{15}$$

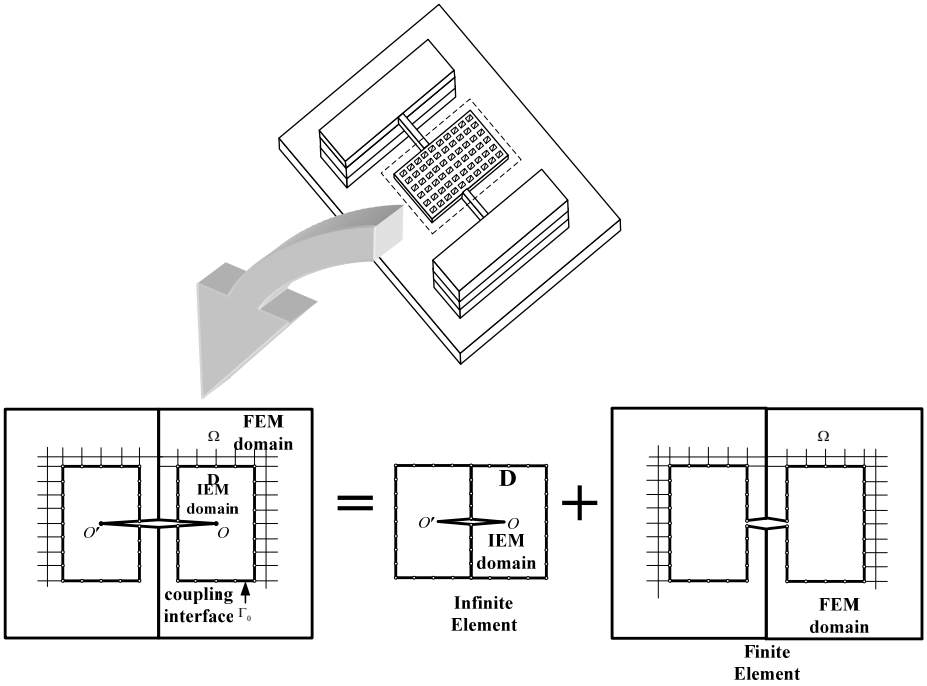

Figure 2: Schematic representation of IE-FE coupled scheme

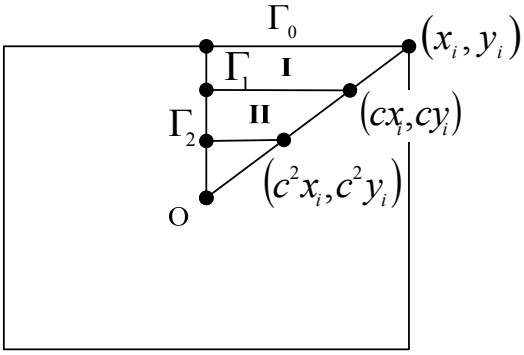

Figure 3: Schematic illustration of similar 2-D elements

$$\begin{cases} x^{II} = cx^{I} = \sum_{i=1}^{4} \phi_i x_i^{II} = c\sum_{i=1}^{4} \phi_i x_i^{I} \\ y^{II} = cy^{I} = \sum_{i=1}^{4} \phi_i y_i^{II} = c\sum_{i=1}^{4} \phi_i y_i^{I} \end{cases} \tag{16}$$

$$det[J]^{II} = c^2 det[J]^{I} \tag{17}$$

The relationship between the stiffness and mass matrices of elements I and II, respectively, is shown in Eq.(18). The stiffness matrix of element I can be expressed as shown in Eq.(19).

$$\begin{cases} k^{II} = k^{I} \\ M^{II} = c^2 M^{I} \end{cases} \tag{18}$$

$$\begin{cases} [k]^{I} = \begin{bmatrix} K_0 & -A^T \\ -A & K_0' \end{bmatrix} \\ [M]^{I} = \begin{bmatrix} L_0 & -D^T \\ -D & L_0' \end{bmatrix} \end{cases} \tag{19}$$

The first layer eigenvalue formulation of IEM is defined in the Eq. (20)

$$\{[k] - \lambda [M]\} \{X\} = 0 \tag{20}$$

where

$$\{X\} = \begin{Bmatrix} \delta_0 \\ \delta_1 \end{Bmatrix}$$

δ_0: the outermost element layer's displacements of IEM.

In general, the stiffness matrix for k-th layer is shown in Eq. (21)

$$\begin{bmatrix} K_0 & -A^T \\ -A & K_0' \end{bmatrix} - \lambda c^{2(k-1)} \begin{bmatrix} L_0 & -D^T \\ -D & L_0' \end{bmatrix} \tag{21}$$

Expanding and arranging the equations for all the layers, the formulations shown in Eq. (22) are obtained. If λ is not an eigenvalue of domain D, then there exists a matrix X(λ) which is a transformation matrix between $\delta 0$ and $\delta 1$, as shown in Eq. (23).

$$(K_0 - \lambda L_0)\,\delta_0 - \left(A^T - \lambda D^T\right)\delta_1 = 0$$

$$-(A - \lambda D)\delta_0 + (K - \lambda L)\,\delta_1 - \left(A^T - \lambda D^T\right)\delta_2 = 0$$

.....

$$-\left(A-\lambda c^{2(k-1)}D\right)\delta_{k-1}+\left(K-c^{2(k-1)}L\right)\delta_k=0$$

$$\left(-A^T+\lambda c^{2k}D^T\right)\delta_{k+1}=0 \tag{22}$$

where $K=K_0+K_0'$, $L=c^2L_0+L_0'$.
$\delta_1=X(\lambda)\delta_0$. $\delta_{k+1}=X\left(\lambda c^{2k}\right)\delta_k$. where

$$X(\lambda)=X_0+\lambda X_1+\cdots+\lambda^m X_m+\ldots. \tag{23}$$

Substituting Eq. (23) into Eq. (22)1 yields the formulation shown in Eq.(24). Arranging the terms in Eq. (24) according to the power of λ, the system shown in Eq. (25) is obtained.

$$-(A-\lambda D)+(K-\lambda L)X(\lambda)-\left(A^T-\lambda D^T\right)X\left(\lambda c^2\right)X(\lambda)=0 \tag{24}$$

$$-A+KX_0-A^TX_0^2=0$$
$$D+KX_1-LX_0-A^T\left(X_0X_1+c^2X_1X_0\right)+c^2D^TX_0^2=0 \tag{25}$$

.....

In general

$$KX_m-LX_{m-1}-A^T\int_{i=0}^{m}c^{2i}X_iX_{m-i}+c^2D^T\int_{i=0}^{m-1}c^{2i}X_iX_{m-i-1}=0$$

where $m=2,3,\ldots.$
All the coefficient terms of X(λ) can be solved using MATLAB. The combined stiffness matrix Kz shown in Eq. (26) is then obtained for domain D.

$$K_z(\lambda)=(K_0-\lambda L_0)-\left(A^T+\lambda D^T\right)X(\lambda)$$

$$K_{IEM}(\lambda)=K_0-A^TX(\lambda)$$
$$M_{IEM}(\lambda)=L_0-D^TX(\lambda) \tag{26}$$

The algebraic assembled element equations for the IE sub-domain are given as follows:

$$[M_{IEM}]\left\{\ddot{X}_0\right\}+[K_{IEM}]\{X_0\}=0$$

$$M_{IEM}=L_0-D^TX(\lambda)$$
$$K_{IEM}=K_0-A^TX(\lambda) \tag{27}$$

where M_{IEM} and K_{IEM} denote the combined mass and stiffness matrices of the IEM sub-domain, respectively.

Clearly, the displacement compatibility condition must be satisfied along the IE-FE interface. Therefore, Eqs.(12) and (27) should be combined as follows:

$$\left[M_{couple}+M_{IEM}\right]\left\{\ddot{X}_0\right\}+M_{cf}^T\left\{\ddot{X}_{FEM}\right\}+\left[K_{couple}+K_{IEM}\right]\left\{X_0\right\}+K_{cf}^T\left\{X_{FEM}\right\}=0 \tag{28}$$

Equations (13) and (28) can then be combined to form the following IE-FE coupled equation:

$$\begin{bmatrix} M_{couple}+M_{IEM} & M_{cf}^T \\ M_{cf} & M_{FEM} \end{bmatrix}\begin{Bmatrix} \ddot{X}_0 \\ \ddot{X}_{FEM} \end{Bmatrix} + \begin{bmatrix} K_{couple}+K_{IEM} & K_{cf}^T \\ K_{cf} & K_{FEM} \end{bmatrix}\begin{Bmatrix} X_0 \\ X_{FEM} \end{Bmatrix}=0. \tag{29}$$

For multiple crack problems, each tip crack can be modeled using an infinite element, which can then be assembled into the global mass and stiffness matrices formed from the FE sub-domain. Significantly, all tip cracks with the same dimensions have the same mass and stiffness matrices. Consequently, the IE matrices need be calculated only once, but can be applied multiple times as required by the number of cracks within the problem domain. In other words, the computational cost and effort of the modeling process are significantly reduced compared to conventional FE methods.

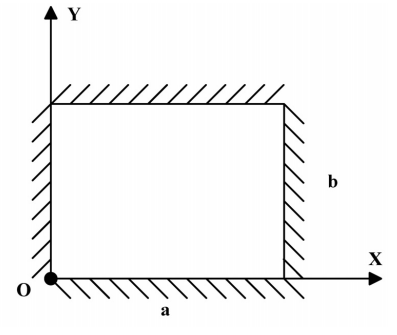

Figure 4: Schematic illustration of reference rectangular membrane model

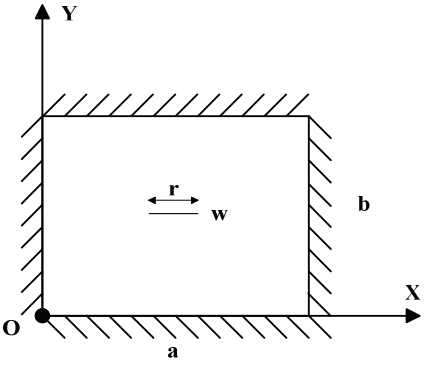

Figure 5: Schematic illustration of center-crack rectangular membrane

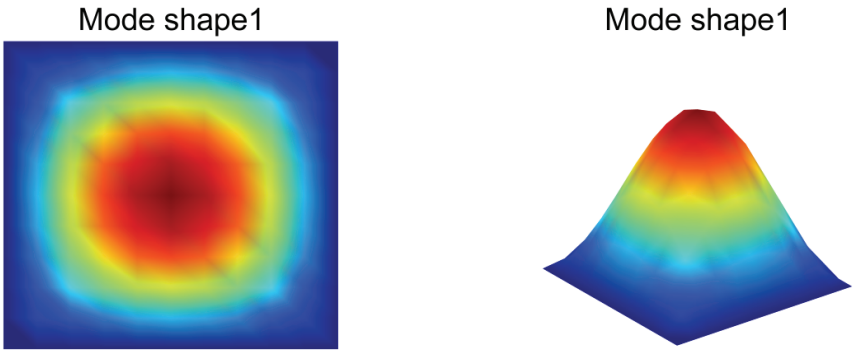

Figure 6: 2-D and 3-D FE modal analysis results for reference rectangular membrane

3 Numerical Case Study I: rectangular membrane

3.1 IE-FE analysis of eigenvalue problem of reference rectangular membrane and center-crack membrane

Consider a rectangular silicon MEMS structure with the following properties: a = 1000 μm, b = 1000 μm, thickness h = 25 μm, tension force per unit edge length T = 3.3 N/mm, and mass density ρ = 2330 kg*m^{-3}. Assume that the membrane is rigidly clamped on all four sides (see Fig. 4) and has natural frequencies and mode shapes. The frequencies of the first four vibration modes can be estimated using the linear theory of transversal vibrations for an elastic membrane (see Eq. (7)).

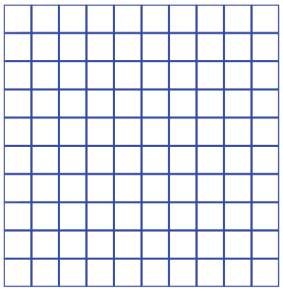

Figure 7: FE mesh for reference rectangular membrane

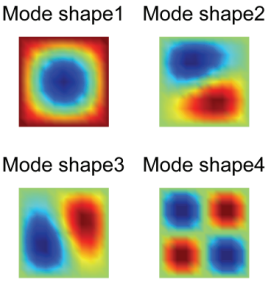

Figure 8: First four mode shapes of reference rectangular membrane

The Finite Element (FE) method is one of the most commonly used numerical methods for predicting the solution of engineering problem. Fig. 6 shows the 2-D and 3-D FE modal analysis results for the wave distribution of the first vibration mode of the reference (i.e., crack-free) membrane shown in Fig. 4. Note that the corresponding FE mesh is shown in Fig. 7. Note also that for convenience, the remaining FE modal analyses presented in this paper are confined to the 2-D view. For example, Fig. 8 presents 2-D views of the first four mode shapes of the reference rectangular membrane. Fig. 5 shows the center-crack membrane model, in which a tip crack with a length of r=50 μm and a width of w=5 μm is positioned symmetrically in the center of the rectangular membrane. The corresponding FE mesh pattern is shown in Fig. 9, while the FE results for the first four mode shapes are shown in Fig. 10.

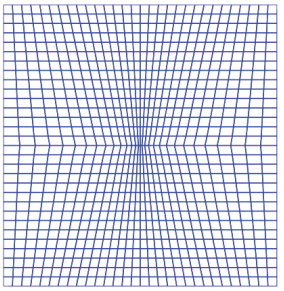

Figure 9: FE mesh for center-crack rectangular membrane

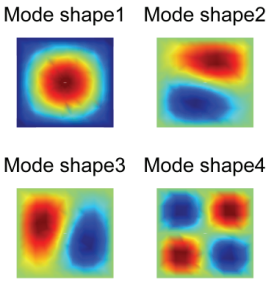

Figure 10: First four mode shapes of center-crack rectangular membrane

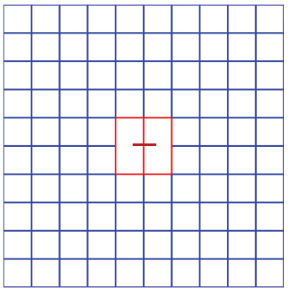

Figure 11: IE and FE mesh pattern for the center crack model

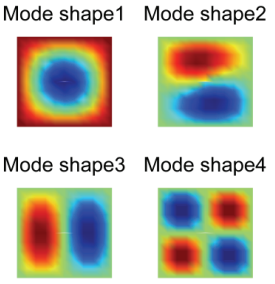

Figure 12: First four mode shape by proposed method of center-crack rectangular membrane

The proposed method solved the central crack problem by coupling the IE and FE method. The mesh pattern is shown in Fig. 11, while the numerical results for the first four mode shapes are shown in Fig. 12. The fundamental frequency is converged in 169.9 kHz. Tab. 1 shows the first four natural frequencies of the reference membrane and center-crack membrane, respectively. It is seen that the FE results for the reference membrane are in close agreement with the theoretical results. In addition, it is observed that there is very little difference in the FE results for the reference model and the center-crack model, respectively. In other words, the presence of a single symmetrical center crack has no obvious effect on the vibration response of the clamped membrane. The proposed scheme is validated by comparing the fundamental frequency (169.6 kHz) with the conventional FE method and theoretical result.

Table 1: Comparison of theoretical and FE results for frequency response of non-cracked and cracked rectangular MEMS membranes (kHz)

Mode	Theory	FEM	Error (%)	Crack	Error (%)
1	168.940	169.636	0.412	169.436	0.294
2	267.118	270.871	1.405	269.694	0.964
3	267.118	270.871	1.405	270.568	1.292
4	337.880	343.462	1.652	343.573	1.685

3.2 IE-FE analysis of frequency response of rectangular membrane with multiple cracks

First, decide the tip crack size and create an infinite element by IEM on the domain which consist of the crack region such like Fig. 13. In accordance with the element similarity concept proposed by Ying, the layered elements within the IE model can be consolidated to a form a "super element" with a combined stiffness matrix of Kz (see Eq. (26)) in section 2-3).

The combined stiffness matrix Kz can then be assembled into the global FE formulation and the corresponding eigenvalue problem solved. As discussed in Section 2-3, the IE stiffness and mass matrices for the super element need be computed only once, but can be applied for every crack in the membrane having the same dimensions.

Fig. 14.1-4a show defect membrane models containing 1, 2, 3 and 4 identical cracks, respectively. Fig. 14.1-4b show the IE-FE analysis results for the first four mode shapes of each model. Tab. 2 shows the first natural frequencies of the reference model and four defect models, respectively. Tab. 3 compares the first four

mode shapes of each of the four defect models with those of the reference model in terms of the MAC-value parameter defined in Eq.(1). The results presented in Tab. 2 and Tab. 3 are consistent with those presented by Brokmann.

Specifically, the number of cracks has no obvious effect on the resonant frequency of the membrane, but crack position impacts the mode shape. That is, the vibration waveform rotates or shifts as the number and position of cracks varies.

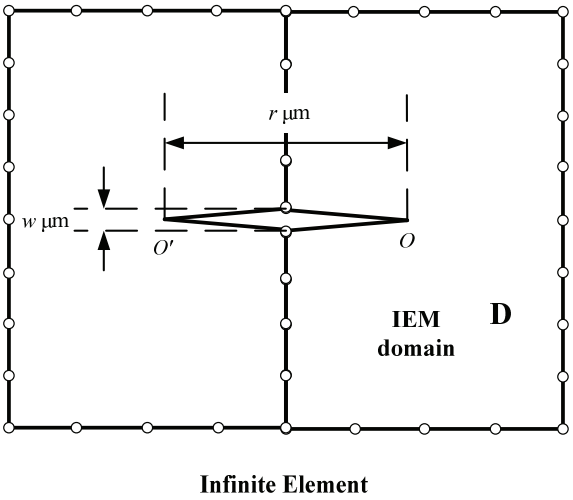

Figure 13: IE model of the tip crack membrane

Table 2: IE-FE results for fundamental frequencies of reference (non-cracked) rectangular MEMS membrane and rectangular MEMS membranes with multiple cracks (kHz).

Mode	Reference	One crack	Two cracks	Three cracks	Four cracks
1	169.6	169.2	168.8	168.5	167.6

3.3 Eigenvalue analysis of multi-crack membranes with different thickness

The thickness of MEMS membranes typically varies in the range of 15 ˜ 65 μm. Fig. 15 shows the IE-FE analysis results for the first four mode shapes of each model. Top side of the figure is the result of the reference model, and the bottom side of the figure is the result of the four-crack model varies in the range of 15 ˜ 65 μm. Tab. 4 compares the results obtained using the FE method and the IE-FE method, respectively, for the fundamental frequency of the four-crack model

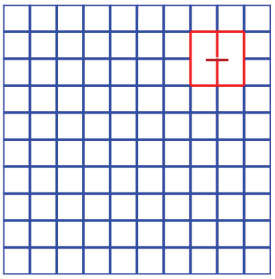

Fig. 14.1a

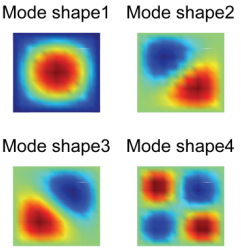

Fig. 14.1b

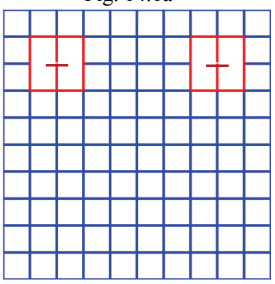

Fig. 14.2a

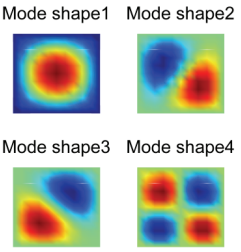

Fig. 14.2b

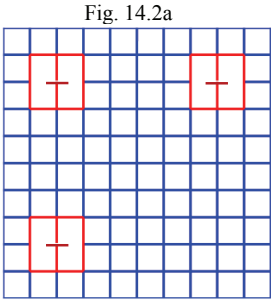

Fig. 14.3a

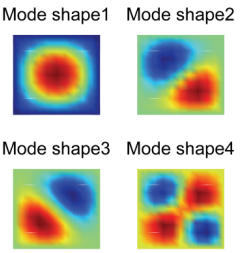

Fig. 14.3b

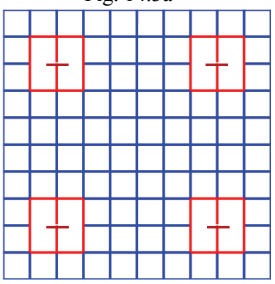

Fig. 14.4a

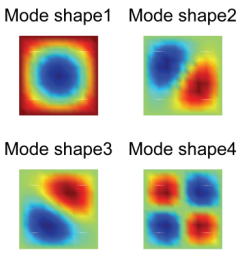

Fig. 14.4b

Figure 14: (a) FE meshes for rectangular MEMS membranes with multiple corner cracks. (b) First four mode shapes of rectangular MEMS membranes with multiple corner cracks.

Table 3: Comparison of mode shapes of rectangular MEMS membranes with multiple cracks with mode shapes of reference (non-cracked) rectangular MEMS membrane (MAC-value, %).

Mode	Reference	One crack	Two cracks	Three cracks	Four cracks
1	100	99.976	99.984	99.984	99.974
2	100	88.308	63.592	88.326	65.426
3	100	84.608	80.720	86.278	65.173
4	100	95.570	93.881	89.473	97.706

given membrane thicknesses of 15, 25, 35, 45, 55 and 65 μm, respectively. From inspection, the difference between the two sets of results is no more than 1.6%. Tab. 5 compares the mode shapes of the first four vibration modes of the four-crack model with the mode shapes of the reference model given membrane thicknesses ranging from 15 ˜ 65 μm. In general, it is difficult to determine the parameters (e.g., thickness) of MEMS devices using direct experimental methods. However, the results presented in Tab. 4 suggest that the IE-FE scheme presented in this study enables the thickness to be inversely (Eq.(30)) derived from the measured values of the resonant frequency given knowledge of the number of cracks in the membrane.

$$h = \frac{\pi^2}{\omega^2}\left[\left(\frac{m}{a}\right)^2 + \left(\frac{n}{b}\right)^2\right]\frac{T}{\rho} \tag{30}$$

Table 4: Comparison of FE and IE-FE results for fundamental frequencies of four-crack rectangular MEMS membranes of different thicknesses (kHz).

Thickness h (μm)	15	25	35	45	55	65
FEM	218.1	169.6	142.7	125.9	113.8	104.7
IEM/ FEM	216.9	167.6	140.8	124.3	112.6	103.4

4 Numerical Case Study II: hollow circular membrane

4.1 Eigenvalue analysis of hollow circular membrane with multiple cracks

Consider the hollow circular membrane model shown in Fig. 16.0a. Assume that the material properties of the membrane are the same as those of the rectangular membrane considered above. Assume also that a fixed boundary condition is applied at all of the outer nodes. The IE-FE analysis results for the first four mode shapes are shown in Fig. 16.0b.

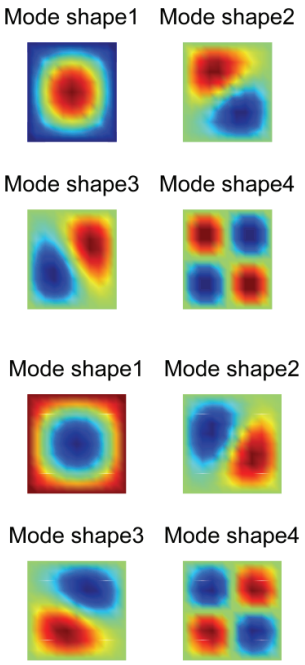

Fig. 15.1 (15μm)

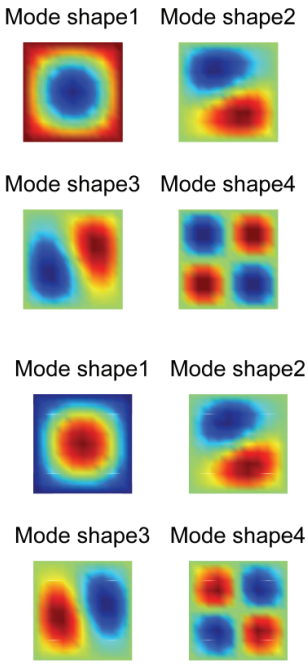

Fig. 15.2 (25μm)

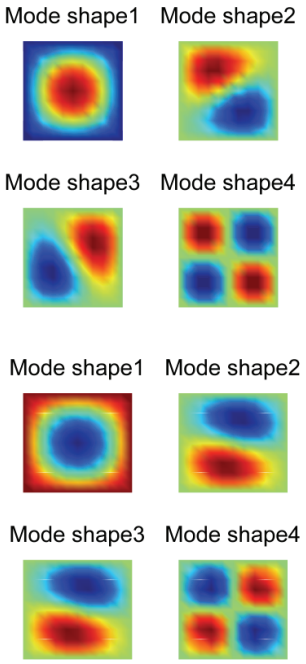

Fig. 15.3 (35μm)

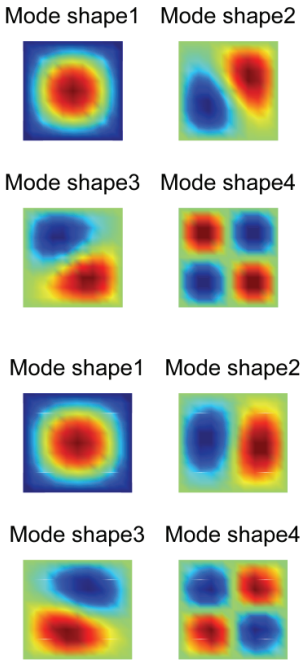

Fig. 15.4 (45μm)

Table 5: Comparison of mode shapes of four-crack rectangular MEMS membranes of various thicknesses with corresponding mode shapes of reference (non-cracked) rectangular MEMS membranes (MAC-value, %).

Mode	Reference	15	25	35	45	55	65
1	100	99.980	99.974	99.968	99.984	99.953	99.963
2	100	71.648	65.426	56.012	65.985	42.497	77.134
3	100	65.763	65.173	43.536	45.483	49.080	70.604
4	100	98.207	97.706	97.168	97.243	98.087	97.835

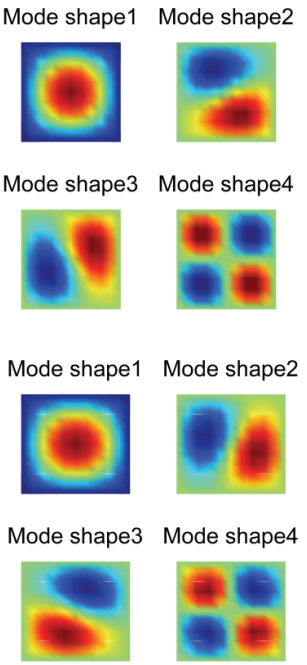

Fig. 15.5 (55µm)

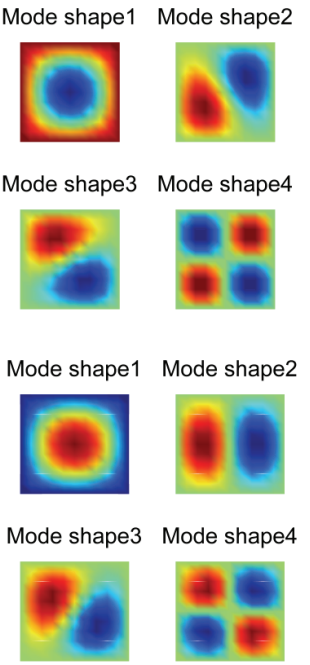

Fig. 15.6 (65µm)

Figure 15: First four mode shapes of four-cracks rectangular MEMS membranes with various thickness

Fig. 16.1-4a show IE-FE defect membrane models containing 1, 2, 3 and 4 identical cracks, respectively. Fig. 16.1-4b show the IE-FE results for the first four mode shapes of each defect model.

Tab. 6 compares the estimated fundamental frequencies of the four defective mem-

branes shown in Fig. 16 with the fundamental frequency of the reference (non-crack) membrane. As for the rectangular membrane, it is seen that the fundamental frequency of the circular membrane is independent of the number of cracks. Tab. 7 compares the first four mode shapes of the four defect membrane models with the corresponding mode shapes of the reference model in terms of the MAC-value.

Table 6: IE-FE results for fundamental frequencies of reference (non-cracked) hollow circular MEMS membrane and hollow circular MEMS membranes with multiple cracks (kHz).

Mode	Reference	One crack	Two cracks	Three cracks	Four cracks
1	102.2	102.0	101.7	101.5	101.2

Table 7: Comparison of mode shapes of hollow circular MEMS membranes with multiple cracks with mode shapes of reference (non-cracked) hollow circular MEMS membrane (MAC-value, %)

Mode	Reference	One crack	Two cracks	Three cracks	Four cracks
1	100	99.989	99.977	99.982	99.992
2	100	99.280	88.384	99.174	65.284
3	100	99.224	88.794	99.234	65.644
4	100	96.794	96.696	96.831	96.928

4.2 Eigenvalue analysis of hollow circular membrane containing single crack with different orientations

Consider a hollow circular membrane containing a single crack (i.e., the scenario shown in Fig. 16.1a in the previous section). In contrast to the conventional FE method, the IE-FE method proposed in this study enables the effect of the crack angle on the frequency response of the membrane to be analyzed without the need to reconstruct the numerical model. Specifically, changes in the crack angle can be modeled simply by rotating the reference point of the super element, as shown in Fig. 17. Fig. 18.1-5a show the IE-FE models for circular membranes with crack rotation angles of 30°, 60°, 90°, 120° and 150°, respectively. The IE-FE results for the first four mode shapes of each model are presented in Fig. 18.1-5b.

Tab. 8 compares the fundamental frequencies of the five crack models shown in Fig. 18 with that of the reference (crack-free) model shown in Fig. 16.0a. It is seen that the crack angle has no obvious effect on the fundamental frequency of the hollow membrane. Tab. 9 compares the mode shapes of the first four frequency modes of

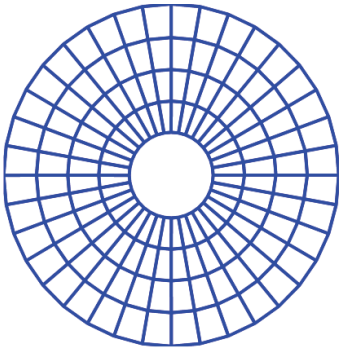

Fig. 16.0a

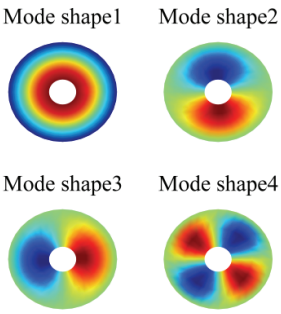

Fig. 16.0b

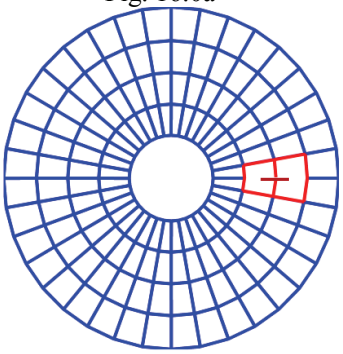

Fig. 16.1a

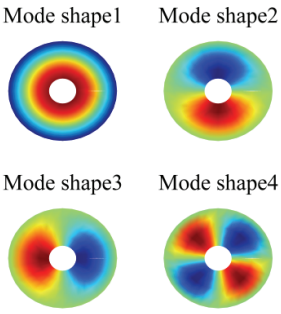

Fig. 16.1b

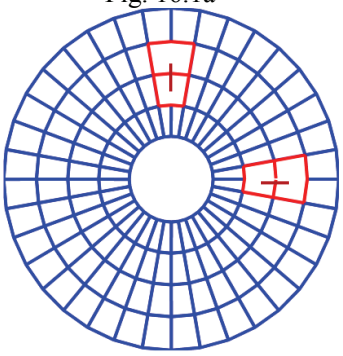

Fig. 16.2a

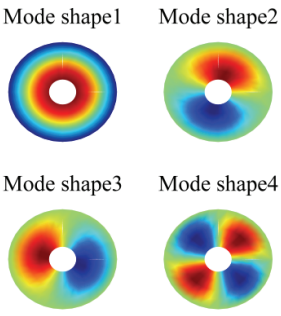

Fig. 16.2b

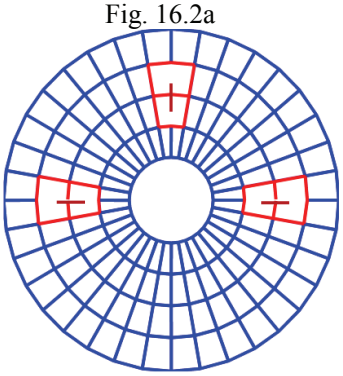

Fig. 16.3a

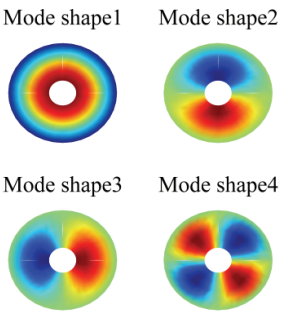

Fig. 16.3b

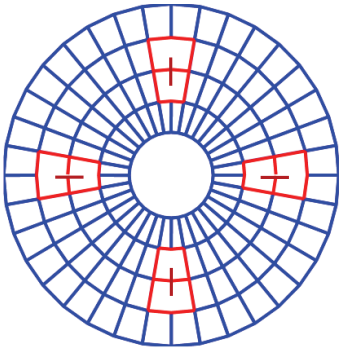

Fig. 16.4a

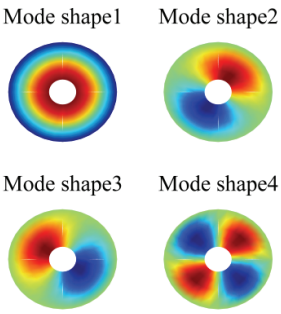

Fig. 16.4b

Figure 16: (a): mesh pattern of the multi-crack on the hollow circular membrane (b): first four mode shapes of the hollow circular membrane model

each crack model with the equivalent mode shapes of the crack-free model. The results show that the angle of the crack has no significant effect on the mode shape for any of the considered frequency modes.

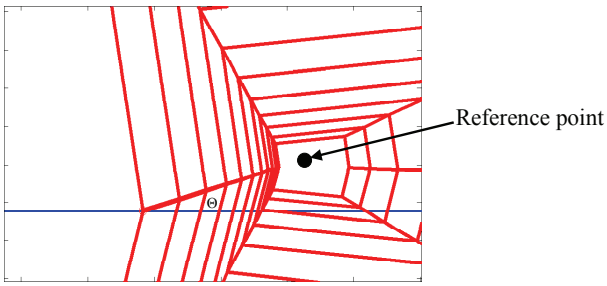

Figure 17: Schematic illustration showing use of reference point rotation in modeling different crack orientations.

Table 8: IE-FE results for fundamental frequencies of reference (non-cracked) hollow circular MEMS membrane and hollow circular MEMS membranes with single cracks orientated at different angles (kHz)

Mode	Reference	30°	60°	90°	120°	150°
1	102.2	101.9	101.9	101.9	101.9	101.9

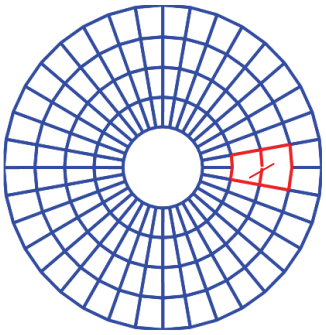

Fig. 18.1a θ=30°

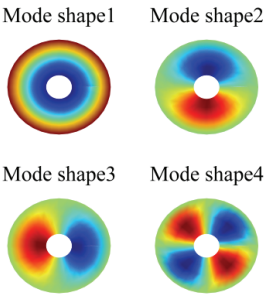

Fig. 18.1b

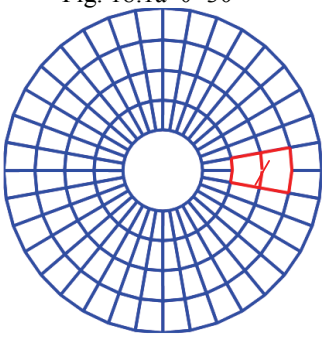

Fig. 18.2a θ=60°

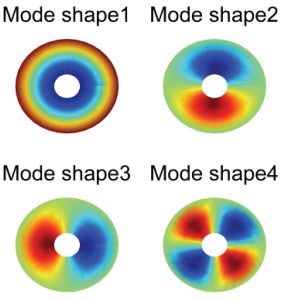

Fig. 18.2b

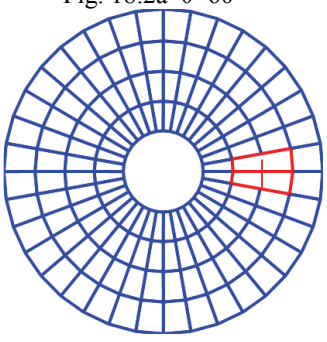

Fig. 18.3a θ=90°

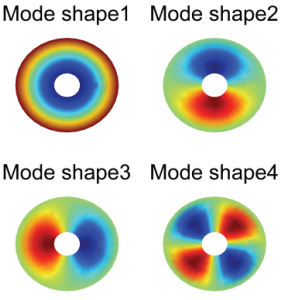

Fig. 18.3b

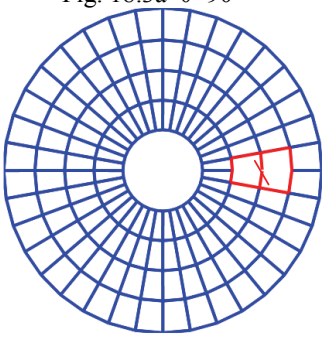

Fig. 18.4a θ=120°

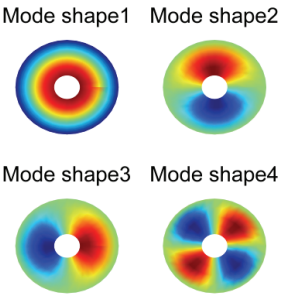

Fig. 18.4b

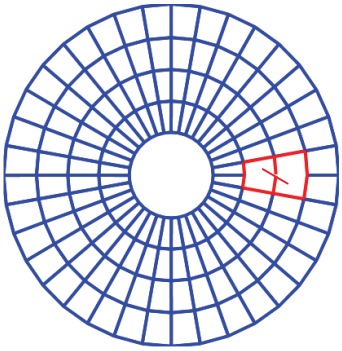

Fig. 18.5a θ=150°

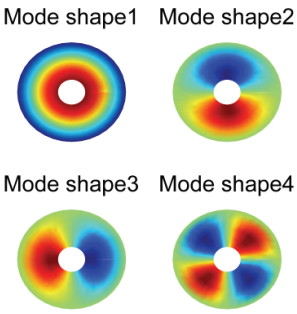

Fig. 18.5b

Figure 18: (a) FE mesh patterns for hollow circular MEMS membrane containing single crack with different orientations. (b) First four mode shapes of hollow circular MEMS membrane containing single crack with different orientations.

Table 9: Comparison of mode shapes of hollow circular MEMS membranes with single cracks orientated at different angles with mode shapes of reference (non-cracked) hollow circular MEMS membrane (MAC-value, %)

Mode	Reference	30°	60°	90°	120°	150°
1	100	99.984	99.981	99.986	99.969	99.978
2	100	98.004	97.713	98.967	99.807	99.846
3	100	97.968	97.666	98.861	99.920	99.776
4	100	96.274	96.142	96.690	97.768	97.489

5 Conclusion

This paper has presented an elegant algorithm based on the Infinite Element Method (IEM) for analyzing the out-of-plane vibration response of MEMS membranes containing one or more cracks. In the proposed approach, a similarity-based partitioning method is used to generate a multi-layered arrangement of infinitesimal elements positioned symmetrically around a central reference point in the IE domain. The individual element layers are then condensed to form a single IE super element with master nodes at the boundary only. Significantly, the IE super element can be applied to all regions of the problem domain containing a crack of the same dimensions and orientation. In other words, there is no need to re-mesh the problem domain each time an additional crack is considered. Consequently, the time and cost of the modeling and analysis processes are significantly reduced. The

proposed IEM algorithm has been coupled with an FE scheme to analyze various cracked membrane vibration problems. The numerical results have shown that the magnitude of the MAC-value provides an effective means of locating the position of the cracks in the membrane. Furthermore, the thickness of the membrane can be inversely derived from the measured fundamental frequency of the membrane.

Overall, the results presented in this study show that the proposed IEM method provides a rapid and efficient means of predicting the effects of manufacturing defects (i.e., cracks) on the dynamic response of MEMS membranes. Furthermore, the algorithm can be easily integrated with experimental frequency measurement methods in order to inversely detect the presence of defects within MEMS membrane structures.

Acknowledgement: The authors gratefully acknowledge the financial support provided to this study by the National Science Council of Taiwan, R. O. C., under Grant Nos. NSC98-2627-E-194-001 and NSC100-2221-E-194-018.

Reference

Ebert, M.; Gerbach, R.; Bagdahn, J.; Michael, S.; Hering, S. (2006): Numerical identification of geometric parameters from dynamic measurement of grinded membranes on wafer level, *Thermal, Mechanical and Multiphysics Simulation and Experiments in Micro-Electronics and Micro-Systems, EuroSimE 2006.*

Ebert, M.; Naumann, F.; Gerbach, R.; Bagdahn, J. (2007): Measurement of dynamic properties of MEMS and the possibilities of parameter identification by simulation. *EuroSimE 2007*, pp. 760–764.

Gerbach, R.; Ebert, M.; Brokmann, G. (2010): Identification of mechanical defects in MEMS using dynamic measurements for application in production monitoring. *Microsyst Technol*, vol. 16, pp. 1251–1257.

Han, H. (1982): The error estimates for the Infinite Element Method for eigenvalue problems. *Analyse Numerique/Numerical Analysis*, vol. 16, pp. 113-128

Han, H. (1983): The Infinite Element Method for eigenvalue problems. *J. Sys. Sci & Math. Scis*, vol. 3, pp. 163-17

Liu, K.Y.; Long, S.Y.; Li, G.Y. (2008): A meshless local Petrov-Galerkin Method for the analysis of cracks in the isotropic functionally graded material, *CMC: Computers, Materials & Continua*, vol. 7, pp. 3-57.

Liu, D.S.; Chiou, D.Y. (2003): A coupled IEM/FEM approach for solving elastic problems with multiple cracks. *International Journal of Solids and Structures,* vol. 40, pp. 1973-1993.

Liu, D.S.; Chiou, D.Y. (2003): 3D IEM formulation with an IEM/FEM coupling scheme for solving elastostatic problems. Advances in Engineering Software, vol. 34, pp. 309-320.

Liu, D.S.; Chiou, D.Y. (2005): 2D infinite element modeling for elastostatic problems with geometric singularity and unbounded domain. *Computer and Structure*, vol. 83, pp. 2086-2099.

Liu, D.S.; Zhuang, Z.W.; Chung, C.L.; Chen, C.Y. (2009): Modeling of moisture diffusion in heterogeneous epoxy resin containing multiple randomly distributed particles using Hybrid Moisture Element Method, *CMC: Computers, Materials & Continua*, vol. 13, pp. 89-113.

Michael, S.; Hering, S.; Holzer, G.; Polster, T.; Hoffmann, M.; Albrecht, A. (2007): Parameter identification on wafer level of membrane structures, *Thermal, Mechanical and Multiphysics Simulation and Experiments in Micro-Electronics and Micro-Systems, EuroSimE 2007.*

Nishioka, T.; Tchouikov, S.; Fujimoto, T. (2006): Numerical investigation of the multiple dynamic crack branching phenomena, *CMC: Computers, Materials & Continua*, vol. 3, pp. 147-153.

Pugno,N.; Peng, B.; Espinosa, H.D. (2004): Predictions of strength in MEMS components with defects — a novel experimental–theoretical approach, *International Journal of Solids and Structures,* vol. 42, pp. 647-661.

Ramakrishnam, N.; Rao, P.R. (2005): An FEM study on crack tip blunting in ductile fracture initiation, *CMC: Computers, Materials & Continua*, vol. 2, pp. 163-176.

Ricart, J.; Blokhina, E.; Gorreta, S. (2010): Control of MEMS Vibration Modes With Pulsed Digital Oscillators—Part II: Simulation and Experimental Results, *IEEE Transactions on Circuits and Systems*, vol. 57, pp. 1879-1890.

Tanner, D.; Walraven, J.; Helgesen, K. (2000): MEMS reliability in a vibration environment. *IEEE, 38th Annualln temational Reliabilii Physics Symposium*, pp. 139–145.

Ying, L.A. (1995): *Infinite Element Method*, Peking University Press, Beijing, and Vieweg Publishing.

Ying, L.A. (1992): An introduction to infinite element method. *Mathematics in Practice Theory,* vol. 2, pp. 69–78.

Zhang, L.M.; Uttamchandani, D.; Culshaw, B.; Dobson, P. (1990): Measurement of Youngs's modulus and internal stress in silicon microresonators using a resonant frequency technique. *Microsyst Technol*, vol. 1, pp. 1343-1346.